ELSEVIER

jmr&t
Journal of Materials Research and Technology
www.jmrt.com.br

abm

Original Article

Fabrication characteristics and mechanical behaviour of rice husk ash – Alumina reinforced Al-Mg-Si alloy matrix hybrid composites

Keneth Kanayo Alaneme[a,*], *Idris B. Akintunde*[a], *Peter Apata Olubambi*[b], *Tolulope M. Adewale*[c]

[a]*Department of Metallurgical and Materials Engineering, Federal University of Technology, Akure, Nigeria*
[b]*Department of Chemical and Metallurgical Engineering, Tshwane University of Technology, Pretoria, South Africa*
[c]*School of Materials, Faculty of Engineering and Physical Sciences, University of Manchester, Manchester, United Kingdom*

ARTICLE INFO

Article history:
Received 29 October 2012
Accepted 26 November 2012

Keywords:
Hybrid composites
Rice husk ash
Al-Mg-Si alloy
Stir casting
Mechanical properties
Microscopy

A B S T R A C T

The fabrication characteristics and mechanical behaviour of Al-Mg-Si alloy matrix composites reinforced with alumina (Al_2O_3) and rice husk ash (RHA, an agro-waste) was investigated. This was aimed at assessing the viability of developing high performance Al matrix composites at reduced cost. Al_2O_3 particulates added with 0, 2, 3, and 4 wt% RHA were utilized to prepare 10 wt% of the reinforcing phase with Al-Mg-Si alloy as matrix using two-step stir casting method. Density measurement, estimated percent porosity, tensile testing, micro-hardness measurement, optical microscopy, and SEM examination were used to characterize the composites produced. The results show that the less dense Al-Mg-Si/RHA/Al_2O_3 hybrid composites have estimated percent porosity levels as low as the single Al_2O_3 reinforced grade (< 2.3% porosity). The hardness of the hybrid composites decreases slightly with increase in RHA content with a maximum reduction of less than 11% observed for the Al-4 wt% RHA-6wt% Al_2O_3 composition (in comparison with the Al-10 wt% Al_2O_3 single reinforced composition). Tensile strength reductions of 8% and 13%, and specific strengths which were 3.56% and 7.7% lower were respectively observed for the 3 wt% and 4 wt% RHA containing hybrid composites. The specific strength, percent elongation and fracture toughness of the 2 wt% RHA containing hybrid composite was however, higher than that of the single Al_2O_3 reinforced and other hybrid composite compositions worked on. RHA thus has great promise to serve as a complementing reinforcement for the development of low cost-high performance aluminum hybrid composites.

*Corresponding author.
E-mail address: kalanemek@yahoo.co.uk (K.K. Alaneme).

2238-7854 © 2013 Brazilian Metallurgical Materials and Mining Association Published by Elsevier Editora Ltda.

http://dx.doi.org/10.1016/j.jmrt.2013.03.012

1. Introduction

This work is a contribution to efforts aimed at the development of Aluminum matrix composites (AMCs) with high performance indices at reduced cost. The well acknowledged good performance in service and consequent high demand for AMCs is attributed to its excellent combination of properties such as high specific strength and stiffness, low thermal coefficient of expansion, good wear, corrosion and high temperature resistance among others [1-3]. These property combinations are very useful for the design of a wide range of components and parts utilized for automobile and aerospace applications [4]. For example, use of AMCs with high specific strength and stiffness for engine components can contribute significantly to the reduction of the overall weight and fuel consumption of automobiles and aircrafts [5,6]. Particulate ceramic materials such as silicon carbide (3.18 g/cm^3) and alumina (3.9 g/cm^3) have been widely utilized as reinforcement in AMCs [7]. These reinforcements are however, denser than Aluminum (2.7 g/cm^3) and thus result in increase in the weight of Aluminum based composites depending on the weight percent of the reinforcing phase [8]. Synthetic reinforcements such as silicon carbide (SiC) and alumina (Al_2O_3) despite their apparent wide spread use, are not produced in most developing countries. The reliance on importation from abroad and the high foreign currency exchange involved implies that the synthetic reinforcements are purchased locally at relatively high cost. A low cost option currently explored by composite materials researchers from developing countries is the consideration of ashes obtained from the controlled burning of agro-wastes such as baggase, rice husk, coconut shell, bamboo leaf and ground nut shell as particulates reinforcement for the development of AMCs [9,10]. These agro-waste ashes often contain a high percentage of silica (SiO_2) with a distribution of other refractory oxides such as Al_2O_3 and hematite (Fe_2O_3) [10,11]. The agro-waste ashes are characterized with densities far lower than that of SiC (3.18 g/cm^3) and Al_2O_3 (3.9 g/cm^3); but the strength levels achieved using these ashes as reinforcement in aluminum matrices is marginal even for high volume percents of the reinforcement [12]. This is due largely to the presence of SiO_2 which is the predominant constituent of agro-waste ashes. SiO_2 has elastic modulus of about 60-70 GPa which is within the same range as that of Aluminum (60 GPa), as compared to the elastic modulus of Al_2O_3 (300-375 GPa) and SiC (410-450 GPa) [13,14]. The agro-waste ashes are thus unlikely to be considered as whole reinforcement for development of AMCs for high stress bearing applications. Harnessing of the light weight and low cost of processing of agro-waste ashes and the high strength of synthetic reinforcements such as Al_2O_3 and SiC for the production of hybrid AMCs is yet to attract much attention from researchers. This research is motivated by the potential benefits of developing high performance AMCs making use of agro-waste ashes as complementary reinforcement to either Al_2O_3 or SiC. In the present study, the fabrication characteristics and mechanical behaviour of Al-Mg-Si alloy matrix hybrid composites developed using rice husk ash (RHA) and Al_2O_3 as complementing reinforcements are reported. The use of RHA in this study is informed by its very low density (0.3-1.6 g/cm^3) in comparison to Al_2O_3 (3.9 g/cm^3), its large availability and even distribution in most part of the world, and its cheap and simple processing requirement [13].

2. Materials and method

2.1. Materials

The base material for the investigation is wrought Al-Mg-Si alloy as received in form of slabs. The chemical composition of the aluminum alloy was determined using a spark spectrometric analyzer and the result is presented in Table 1. All (100%) chemically pure Al_2O_3 particles having particle size of 28 μm and rice husk obtained from Igbemo-Ekiti, Ekiti State (a rice producing community in south western Nigeria) were utilized as reinforcing particulates. Magnesium for improvement of wettability between the Al-Mg-Si alloy and the reinforcements was also procured.

2.2. Method

2.2.1. Preparation of rice husk ash

A simple metallic drum with perforations to allow for air circulation to aid combustion was used as burner for the preparation of the RHA. Dry rice husks were placed inside the drum while charcoal which served as the fire source was used to ignite the rice husk. The husk was left to burn completely and the ashes removed 24 hours later. The ash was then conditioned by heat-treating the ash at a temperature of 650 °C for 180 minutes to reduce the carbonaceous and volatile constituents of the ash [13]. The chemical composition of the RHA is presented in Table 2.

2.2.2. Composites production

Two steps stir casting process performed in accordance with Alaneme and Aluko [15] were utilized to produce the

Table 1– Elemental composition of Al-Mg-Si alloy.

Element	wt%
Si	0.4002
Fe	0.2201
Cu	0.0080
Mn	0.0109
Mg	0.3961
Cr	0.0302
Zn	0.0202
Ti	0.0125
Ni	0.0101
Sn	0.0021
Pb	0.0011
Ca	0.0015
Cd	0.0003
Li	0.0000
Na	0.0009
V	0.0027
Al	98.88

Table 2 – Chemical composition of the rice husk ash.

Compound/element (constituent)	wt%
Silica (SiO_2)	91.56
Carbon, C	4.8
Calcium oxide, CaO	1.58
Magnesium oxide, MgO	0.53
Potassium oxide, K_2O	0.39
Haematite, Fe_2O_3	0.21
Silver, Ag	trace

composites. The process started with the determination of the quantities of RHA and Al_2O_3 required to produce 10 wt% reinforcement consisting of 0:10, 2:8, 3:7, and 4:6 RHA and Al_2O_3 wt%, respectively. The RHA and Al_2O_3 particles were initially preheated at a temperature of 250 °C to remove moisture and to help improve wettability with the Al-Mg-Si alloy melt. The Al-Mg-Si alloy ingots were charged into a gas-fired crucible furnace and heated to a temperature of 750 °C ± 30 °C (above the liquidus temperature of the alloy) and the liquid alloy was then allowed to cool in the furnace to a semi solid state at a temperature of about 600 °C. The preheated RHA and Al_2O_3 particulates along with 0.1 wt% magnesium were added at this temperature and stirring of the slurry was performed manually for 5-10 minutes. The composite slurry was then superheated to 800 °C ± 30 °C and a second stirring performed using a mechanical stirrer. The stirring operation was performed at a speed of 400 rpm for 10 minutes to help improve the distribution of the particulates in the molten Al-Mg-Si alloy. The molten composite was then cast into prepared sand moulds inserted with chills.

2.2.3. Density measurement

Density measurements were carried out to study the effect of the RHA-Al_2O_3 wt% proportions on the densities of the composites produced. The measured (experimental) density was also used to estimate the porosity levels in the composites. This was achieved by comparing the experimental and theoretical densities of each weight ratio of RHA-Al_2O_3 reinforced composite produced [16]. The experimental density for each composite was evaluated by weighing the test sample using a high precision electronic weighing balance with a tolerance of 0.1 mg. The measured weight in each case was divided by the volume of the respective sample. The theoretical density was evaluated by using the rule of mixtures given by:

$$\rho_{Al\text{-}Mg\text{-}Si/RHA\text{-}Al_2O_{3p}} = wt._{Al\text{-}Mg\text{-}Si} \times \rho_{Al\text{-}Mg\text{-}Si} + wt._{RHA} \times \rho_{RHA} + wt._{Al_2O_3} \times \rho_{Al_2O_3} \quad (2.1)$$

where $\rho_{Al\text{-}Mg\text{-}Si/RHA\text{-}Al_2O_{3p}}$ is the density of composite, $wt._{Al\text{-}Mg\text{-}Si}$ represents the weight fraction of Al-Mg-Si alloy, $\rho_{Al\text{-}Mg\text{-}Si}$ is the density of Al-Mg-Si alloy, $wt._{RHA}$ is the weight fraction RHA, ρ_{RHA} rerpresents density of RHA, $wt._{Al_2O_3}$ is the weight fraction Al_2O_3, and $\rho_{Al_2O_3}$ is the density of Al_2O_3.

The percent porosity of the composites was estimated using the relations [16]:

$$\% \text{ porosity} = \{(\rho_T - \rho_{EX}) \div \rho_T\} \times 100\% \quad (2.2)$$

where ρ_T is the theoretical density (g/cm^3) and ρ_{EX} is the experimental density (g/cm^3).

2.2.4. Mechanical test

Room temperature uniaxial tension tests were performed on round tensile samples machined from the prepared composites with dimensions of 6 mm diameter and 30 mm gauge length. The testing was performed using an instron universal testing machine operated at a constant cross head speed of 1 mm/s. The specimen dimension specifications and the test procedure adopted were in conformity with ASTM E8M-91 standards [17]. Three tests were performed for each composite composition to guarantee reliability of the data generated. The tensile properties evaluated from the stress-strain curves developed from the tension test are – the ultimate tensile strength (σ_u), the 0.2% offset yield strength (σ_y), and the strain to fracture (ε_f).

Circumferential notch tensile (CNT) specimens were also prepared for the evaluation of fracture toughness in accordance with Alaneme [18]. The CNT specimens were machined with gauge length of 30 mm, specimen diameter of 6 mm (D), notch diameter of 4.5 mm (d) and notch angle of 60°. The specimens were then subjected to tensile loading to fracture using an instron universal testing machine. The fracture load (P_f) obtained from the CNT specimens' load – extension plots were used to evaluate the fracture toughness using the empirical relations by Dieter [19]:

$$K_{1C} = P_f / (D)^{3/2} [1.72(D/d) - 1.27] \quad (2.3)$$

where, D and d are respectively the specimen diameter and the diameter of the notched section. The validity of the fracture toughness values was evaluated using the relations in accordance with Nath and Das [20]:

$$D \geq (K_{1C}/\sigma_y)^2 \quad (2.4)$$

A minimum of two tests were performed for each composite composition and the results obtained were taken to be highly consistent if the difference between measured values for a given composite composition is not more than 2%.

The hardness of the composites was evaluated using an EmcoTEST DURASCAN Microhardness Tester equipped with ecos workflow ultra modern software. Prior to testing, test specimens cut out from each composite composition were polished to obtain a flat and smooth surface finish. A load of 100 g was applied on the specimens and the hardness profile was evaluated following standard procedures. Multiple hardness tests were performed on each sample and the average value taken as a measure of the hardness of the specimen.

2.2.5. Microstructural characterization

A Zeiss Metallurgical Microscope with accessories for image analysis was used for optical microscopic investigation of the composites produced. The specimens for the test were metallographically polished and etched with 1HNO3:1HCl solution before microscopic examination was performed. A JSM 7600F Jeol ultra-high resolution field emission gun scanning electron microscope (FEG-SEM) equipped with an EDS was

used for detailed study of the microstructural features of the specimens and also for determination of the qualitative elemental composition of the composites.

3. Result and discussion

3.1. *Microstructure*

Fig. 1 shows some representative optical micrographs for the RHA-Al_2O_3 reinforced AMCs produced. It is observed that the RHA and Al_2O_3 particulates are visible and a good dispersion of the particulates in the Aluminum matrix is evident. It is also observed from Fig. 1b that there is a high volume percent of particulates dispersed in the aluminum matrix for the hybrid composite containing 4 wt% of the RHA in comparison to the single reinforced Al-Mg-Si/10 wt% Al_2O_3 composite (Fig. 1a).

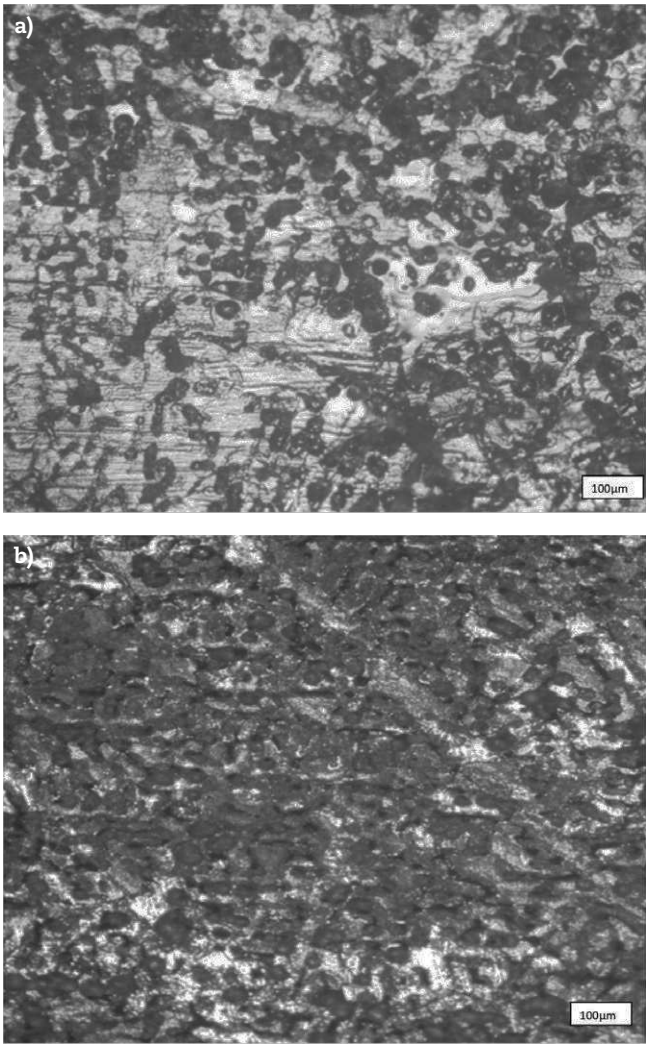

Fig. 1 – a) Photomicrograph of the Al-Mg-Si/10 wt% Al_2O_3 composite showing the Al_2O_3 particles dispersed in the Al-Mg-Si matrix. b) Photomicrograph of the Al-Mg-Si/4wt% rice husk ash-6 wt% Al_2O_3 hybrid composite showing a high density of particles dispersed in the Al-Mg-Si matrix.

This is due to the higher volume percent of the RHA arising from its very low density (0.31 g/cm^3) in comparison with Al_2O_3 (3.18 g/cm^3).

The representative SEM micrographs and EDS profiles of the Al-Mg-Si/2 wt%RHA-8 wt% Al_2O_3 and Al-Mg-Si/3 wt% RHA-7 wt% Al_2O_3 hybrid composites are presented in Figs. 2 and 3. Figs. 2a and 3a confirm that the reinforcing particulates are dispersed in the Aluminum matrix. The EDS profiles (Figs. 2b and 3b) show peaks of aluminum (Al), oxygen (O), carbon (C), iron (Fe), silicon (Si), and traces of silver (Ag). The presence of oxygen confirms the presence of SiO_2, Al_2O_3, potassium oxide and ferric oxide (Fe_2O_3), which are the constituents derived from the RHA.

3.2. *Composite density and estimated percent porosity*

The results of the estimated percent porosity of the composites are presented in Table 3. It is observed from comparison of the theoretical and experimental densities of the composites that slight porosities (less than 2.3%) exist in the produced composites. The values are however lower than 4% which is the

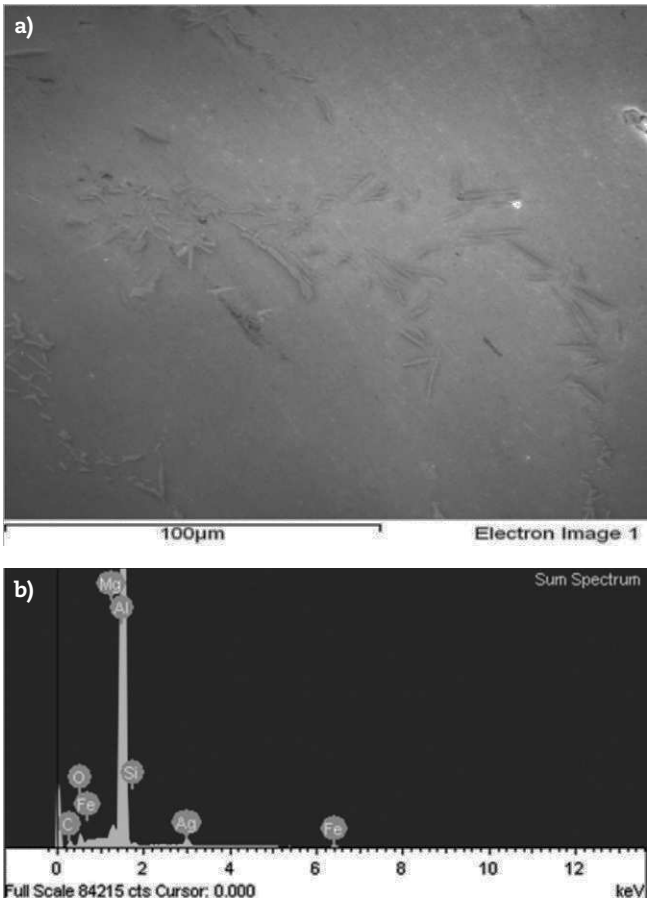

Fig. 2 – a) Representative SEM photomicrograph of the Al-Mg-Si/2wt% rice husk ash-8 wt% Al_2O_3 hybrid composite showing particles dispersed in the Al-Mg-Si matrix. b) EDAX profile obtained from the Al-Mg-Si/2wt% rice husk ash-8 wt% Al_2O_3 hybrid composite confirming the presence of Al_2O_3, SiO_2, Fe_2O_3, K_2O, C, and Ag.

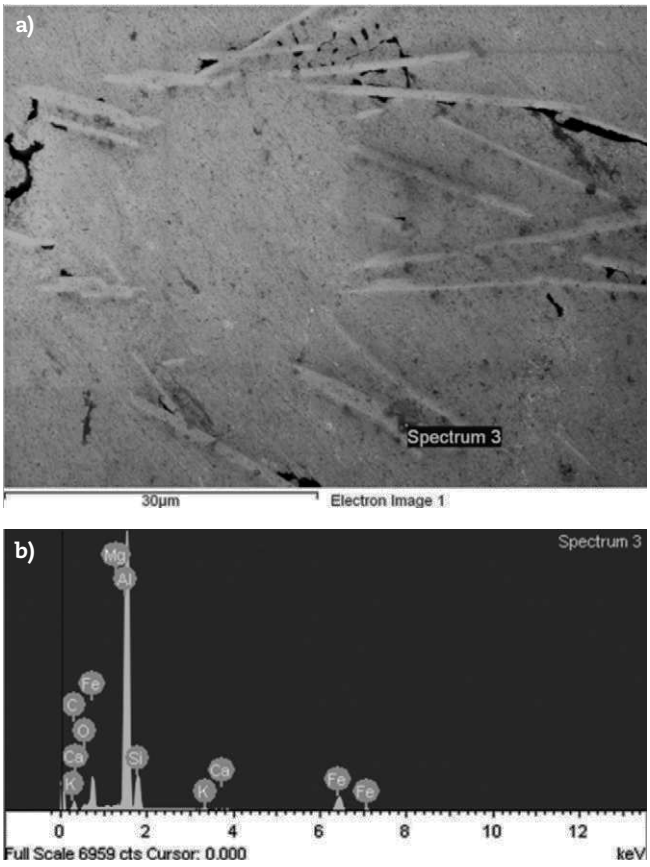

Fig. 3 – a) Representative scanning electron microscope photomicrograph of the Al-Mg-Si/3wt% rice husk ash-7 wt% Al_2O_3 hybrid composite showing particles dispersed in the Al-Mg-Si matrix. b) EDAX profile obtained from the particle indentified in (a) confirming the presence of Al_2O_3, SiO_2, Fe_2O_3, K_2O, Cao, and C which are known constituents of rice husk ash.

maximum porosity level reported to be acceptable in cast AMCs [15,21]. The low porosity levels observed is a good indicator of the reliability of the two step stir casting process utilized for the production of the hybrid composites. As expected, the densities of the hybrid composites reduce with increase in the weight percent of RHA that constitutes the reinforcement. In comparison with the composite having 10 wt% Al_2O_3, the hybrid composites consisting of 2 wt% RHA-8 wt% Al_2O_3, 3 wt% RHA-7 wt% Al_2O_3 and 4 wt% RHA-6 wt% Al_2O_3, had 3.76%, 4.66% and 5.91% reduction in densities, respectively. It should be noted that Al_2O_3 is purchased at ~100 US dollars/kg as compared with the processing of the RHA which is ~6.25 US dollars/kg. This gives a cost savings of ~93.75 US dollars/kg if RHA is used in place of Al_2O_3. The above analysis shows that depending on the weight percent rice husk in the hybrid reinforcement, lighter weight AMCs can be produced at significantly reduced cost.

3.3. *Mechanical behavior*

The hardness values of the composites are presented in Fig. 4. It is observed that the hardness decreases slightly with increase in the weight percent of RHA in the hybrid composites. 4.58%, 8.14% and 10.94% reduction in hardness was observed for the hybrid composites having respectively 2, 3 and 4 wt% RHA in comparison with the single reinforced Al-Mg-Si matrix-10wt% Al_2O_3 composite with hardness HRA 78.6. This trend is due to the composition of RHA which consists mainly of SiO_2 which is noted to have a lower hardness level in comparison with Al_2O_3 [22]. Hence the slight decrease in the hardness of the hybrid composites is to be expected.

Fig. 5 shows the variation of ultimate tensile and yield strength with increase in the RHA content of the hybrid composites. It is observed that there is a slight reduction in tensile strength (Fig. 5a) and yield strength (Fig. 5b) with increase in the RHA content in the reinforcement. The decrease in tensile strength was 3.7%, 8% and 13%

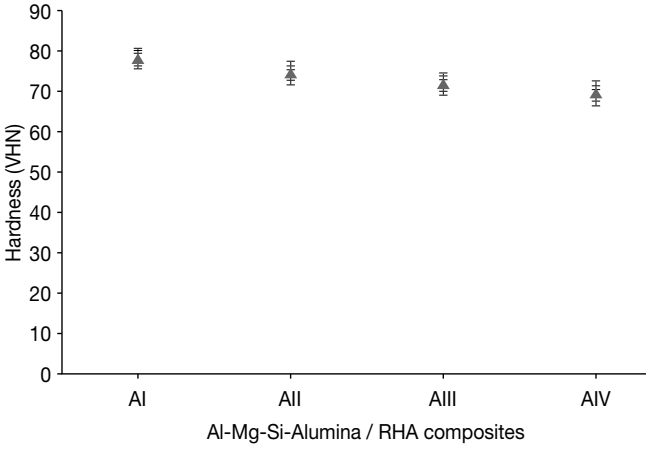

Fig. 4 – Variation of hardness for the single reinforced Al-Mg-Si/10 wt% Al_2O_3 and hybrid reinforced Al-Mg-Si/rice husk ash-Al_2O_3 composites.

Table 3 – Composite density and estimated percent porosity.

Sample designation	Weight ratio of RHA and Al_2O_3	Theoretical density	Experimental density	% porosity
A_I	0:10	2.82	2.791	1.028
A_{II}	2:8	2.749	2.686	2.292
A_{III}	3:7	2.713	2.661	1.917
A_{IV}	4:6	2.678	2.626	1.942

RHA: rice husk ash.

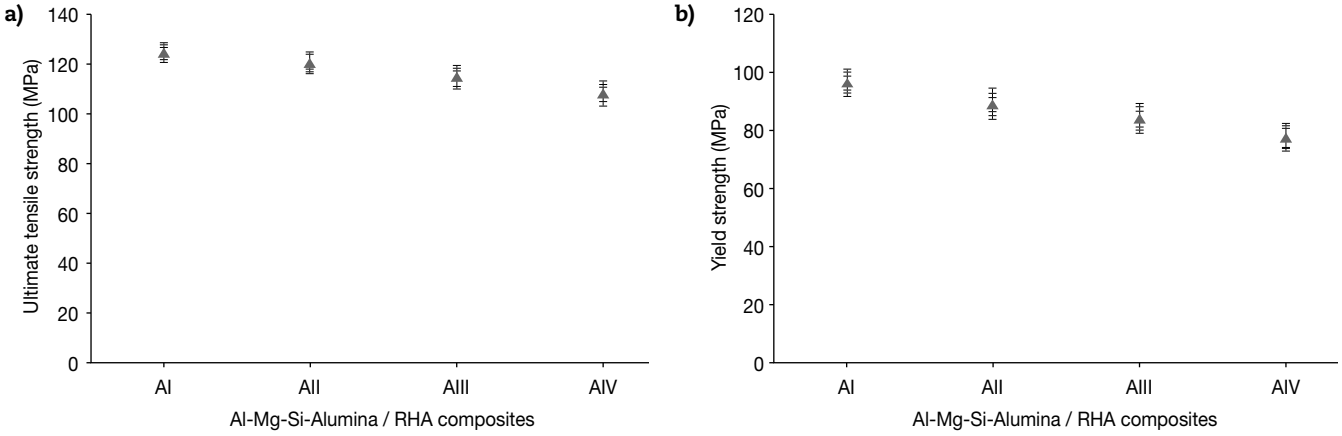

Fig. 5 – a) Variation of tensile strength for the single reinforced Al-Mg-Si/10 wt% Al_2O_3 and hybrid reinforced Al-Mg-Si/ rice husk ash-Al_2O_3 composites. b) Variation of yield strength for the single reinforced Al-Mg-Si/10 wt% Al_2O_3 and hybrid reinforced Al-Mg-Si/rice husk ash-Al_2O_3 composites.

for the hybrid composites containing 2, 3 and 4 wt% RHA in the reinforcement relative to the single reinforced Al-Mg-Si matrix-10wt% Al_2O_3 composite which had UTS of 125.5 MPa. This trend is attributed to a slight reduction in the strengthening capacity expected from load transfer from the matrix to the particulates. It is noted that when hard particulates are used as reinforcement in metal matrix composites (MMCs) there is improvement in the strength due to the synergy of direct and indirect strengthening mechanisms [23]. Chawla and Shen [24] have reported that direct strengthening arises in metal matrix composites as a result of the transfer of load from the weaker matrix to the harder and stiffer particulates through the matrix particulate interface. This will result in increased resistance to plastic deformation and a higher work hardening capacity in MMCs [25]. Indirect strengthening also occurs due to high thermal mismatch arising from uneven cooling between the metallic matrix that has a higher coefficient of expansion and the embedded ceramic particulates with lower coefficient of expansion [26]. The thermal mismatch results in the formation of dislocations at the reinforcement/matrix interface, which contributes to improve the strength of the composite as a result of increased dislocation density in the MMC [24].

However, in the present case the slight decrease in strength observed may be attributed to a reduction in the contribution of the direct strengthening effect. RHA, which is dominantly SiO_2, is a softer particle in comparison with Al_2O_3 and has about the same elastic modulus as aluminum (60-70 GPa) in comparison to Al_2O_3 (250 GPa) [22]. Thus the load carrying capacity of the hybrid particulates will be dependent on the amount of Al_2O_3 rather than RHA. Fig. 6 however shows that the specific strength of the hybrid composite containing 2 wt% RHA (45.5 MPa/g/cm^3) is slightly higher than that of the single reinforced Al-Mg-Si-10 wt% Al_2O_3 (~2% higher). This is in contrast with the 3.7% superior ultimate tensile strength the Al-Mg-Si-10 wt% Al_2O_3 had over the hybrid composite containing 2 wt% RHA discussed earlier. The hybrid composite containing 3 and 4 wt% RHA had respectively 3.56% and 7.7% lower specific strength relative to the single

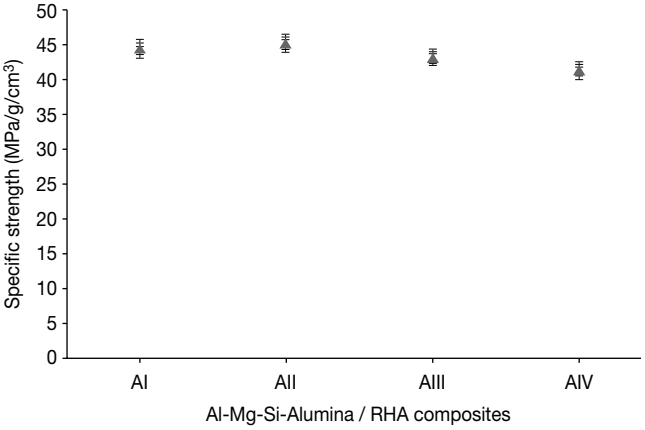

Fig. 6 – Variation of specific strength for the single reinforced Al-Mg-Si/10 wt% Al_2O_3 and hybrid reinforced Al-Mg-Si/rice husk ash-Al_2O_3 composites. RHA: rice husk ash.

reinforced Al-Mg-Si-10 wt% Al_2O_3 composite. This is a modest improvement compared to the 8% and 13% lower UTS values they exhibited when compared with the single Al_2O_3 reinforced composite. This shows that comparable or even higher strength to weight ratios can be achieved using cheap RHA agro waste as a complementing reinforcement for the production of Al_2O_3 reinforced Al matrix composites.

Fig. 7, which is the plot of strain to fracture, shows that higher ductility levels can be achieved with the use of 2 wt% RHA. Higher weight proportions resulted in reduced ductility of the hybrid composites.

The fracture toughness values determined by the use of circumferential notched tensile (CNT) specimens is presented in Fig. 8. The values obtained were reported as plain strain fracture toughness because the conditions for valid K_{1C} (plain strain condition) was met with the specimen diameter of 6 mm when the relation $D \geq (K_{1C}/\sigma_y)^2$ [20] was utilized to validate the results obtained from the CNT

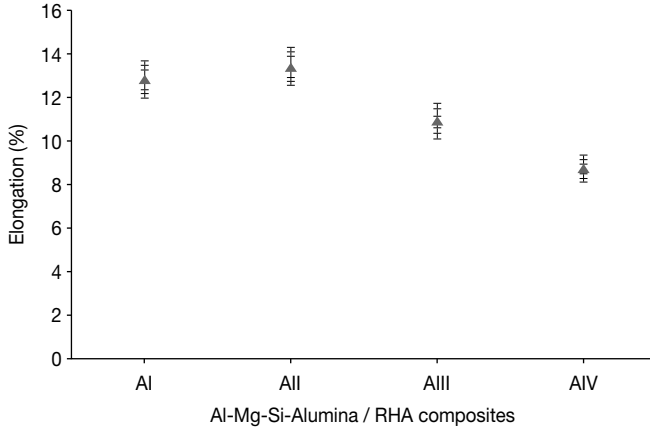

Fig. 7 – Variation of percent elongation for the single reinforced Al-Mg-Si/10 wt% Al_2O_3 and hybrid reinforced Al-Mg-Si/rice husk ash-Al_2O_3 composites. RHA: rice husk ash.

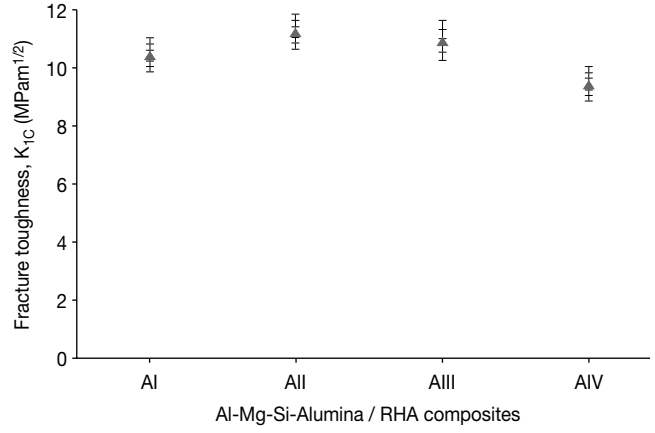

Fig. 8 – Variation of fracture toughness for the single reinforced Al-Mg-Si/10 wt% Al_2O_3 and hybrid reinforced Al-Mg-Si/rice husk ash-Al_2O_3 composites. RHA: rice husk ash.

testing. It is observed that the fracture toughness of the hybrid composites containing 2 and 3 wt% RHA had higher fracture toughness values in comparison with the single Al_2O_3 reinforced composite. The mechanism of fracture in Al matrix composites has been reported by several authors [23,25,26]. The primary mechanisms of fracture have been attributed to particle cracking, interfacial cracking or particle debonding [23]. Ceramic particulates are generally hard and brittle; and like most brittle materials, have a poor tendency to resist rapid crack propagation [27]. In the case of the hybrid composites, the fracture micro-mechanism which could explain the slight improvement in fracture toughness observed in the 2 and 3 wt% RHA containing composites still requires further studies. It is however clear that the addition of 2-3 wt% RHA did not deteriorate the fracture toughness of the Al_2O_3 reinforced Al matrix composites.

4. Conclusions

The fabrication characteristics and mechanical behaviour of Al-Mg-Si alloy matrix composites containing 0:10, 2:8, 3:7 and 4:6 wt% RHA and Al_2O_3 as reinforcement was investigated. The results show that:

- The less dense Al-Mg-Si/RHA/Al_2O_3 hybrid composites have estimated percent porosity levels as low as the single Al_2O_3 reinforced grade (< 2.3% porosity).
- The hardness of the hybrid composites decreases slightly with increase in RHA content with a maximum reduction of less than 11% observed for the Al-4 wt% RHA-6 wt% Al_2O_3 composition (in comparison with the Al-10 wt% Al_2O_3 single reinforced composition).
- Tensile strength reductions of 8% and 13% and specific strengths which were 3.56% and 7.7% lower were respectively observed for the 3 and 4 wt% RHA containing hybrid composites.
- The specific strength, percent elongation and fracture toughness of the 2 wt% RHA containing hybrid composite was higher than that of the single Al_2O_3 reinforced and other hybrid composite compositions worked on.
- RHA has great promise to serve as a complementing reinforcement for the development of low cost-high performance aluminum hybrid composites.

Acknowledgements

The authors wish to recognise the support of the National Research Foundation (NRF) National Nanotechnology Equipment Program (NNEP) (74407).

REFERENCES

[1] Alaneme KK, Bodunrin MO. Corrosion behaviour of alumina reinforced Al (6063) metal matrix composites. JMMCE. 2011; 10:1153-65.
[2] Surappa MK. Aluminum matrix composites: Challenges and opportunities. Sadhana. 2003;28:319-34.
[3] Rohatgi P, Schultz B. Light weight metal matrix composites – stretching the boundaries of metals. Materials Matters. 2007; 2:16-9.
[4] Alaneme KK. Influence of thermo-mechanical treatment on the tensile behaviour and CNT evaluated fracture toughness of borax premixed SiCp reinforced aluminum (6063) composites. Int J Mech Mater Eng. 2012;7:96-100.
[5] Macke A, Schultz BF, Rohatgi P. Metal matrix composites offer the automotive industry an opportunity to reduce vehicle weight, improve performance. Adv Mater Processes. 2012;170: 19-23.
[6] Christy TV, Murugan N, Kumar S. A comparative study on the microstructures and mechanical properties of Al 6061 alloy and the MMC Al 6061/TiB2/12p. JMMCE. 2010;9:57-65.
[7] Miracle DB. Metal matrix composites – from science to technological significance. Compos Sci Technol. 2005;65: 526-40.

[8] Prabu SB, Karanamoorty L, Kathiresan S, Mohan B. Influence of stirring speed and stirring time on distribution of particulates in cast metal matrix composite. J Mater Process Technol. 2006;171:268-73.
[9] Aigbodion VS, Hassan SB, Dauda ET, Mohammed RA. Experimental study of ageing behaviour of Al-Cu-Mg/bagasse ash particulate composites. Tribology in industry. 2011;33:28-35.
[10] Madakson PB, Yawas DS, Apasi A. Characterization of Coconut shell ash for potential utilization in metal matrix composites for automotive applications. IJEST. 2012;4:1190-8.
[11] Olugbenga OA, Akinwole AA. Characteristics of bamboo leaf ash stabilization on lateritic soil in highway construction. IJET. 2010;2:212-9.
[12] Prasad SD, Krishna RA. Production and mechanical properties of A356.2/RHA composites. IJAST. 2011;33:51-8.
[13] Prasad SD, Krishna RA. Tribological properties of A356.2/RHA composites. JMST. 2012;28:367-72.
[14] Zuhailawati H, Samayamutthirian P, Mohd Haizu CH. Fabrication of low cost aluminum matrix composite reinforced with silica sand. J Phys Sci. 2007; 18:47-55.
[15] Alaneme KK, Aluko AO. Production and age-hardening behaviour of borax pre-mixed SiC reinforced Al-Mg-Si alloy composites developed by double stir casting technique. WIJE. 2012;34:80-5.
[16] Alaneme KK. Mechanical behaviour of cold deformed and solution heat-treated alumina reinforced AA 6063 composites. J Eur Ceram Soc. 2013; 35(2):31-5.
[17] ASTM E 8M: Standard test method for tension testing of metallic materials (Metric). Annual Book of ASTM Standards, Philadelphia; 1991.
[18] Alaneme KK. Fracture toughness (K1C) evaluation for dual phase low alloy steels using circumferential notched tensile (CNT) specimens. Mat Res. 2011;14:155-60.
[19] Dieter GE. Mechanical metallurgy. Singapore: McGraw-Hill; 1988.
[20] Nath SK, Das UK. Effect of microstructure and notches on the fracture toughness of medium carbon steel. JNAME. 2006;3: 15-22.
[21] Kok M. Production and mechanical properties of Al_2O_3 particle reinforced 2024 aluminum composites. J Mater Process Technol. 2005;16:381-7.
[22] Courtney TH. Mechanical behaviour of materials. 2nd ed. India: Overseas Press; 2006.
[23] Alaneme KK, Aluko AO. Fracture toughness (K1C) and tensile properties of as-cast and age-hardened aluminum (6063) – Silicon carbide particulate composites. Sci Iran, Trans A. 2012; 19:992-6.
[24] Chawla N, Shen Y. Mechanical behaviour of particle reinforced metal matrix composites. Adv Eng Mater. 2001;3:357-70.
[25] Milan MT, Bowen P. Tensile and fracture toughness properties of SiCp reinforced Al alloys: Effects of particle size, particle volume fraction and matrix strength. J Mater Eng Perform. 2004;13:775-83.
[26] Ranjbaran MM. Low fracture toughness in Al 7191-20% SiCp aluminum matrix composite. Eur J Appl Eng Sci Res. 2010; 41:261-72.
[27] Bradt RC, Munz D, Sakai M, Schevchenko VY, White KW (eds.). Fracture Mechanics of Ceramics, Vol. 13 – Crack-Microstructure Interaction, R-Curve Behaviour, Environmental Effects in Fracture, and Standardization. New York: Springer; 2002.